

# Transport properties of La-doped Mn–Zn ferrite

S. Solyman

*Physics Department, Faculty of Science, Zagazig University, Zagazig, Egypt*

Received 13 January 2005; received in revised form 21 April 2005; accepted 25 May 2005

Available online 18 August 2005

## Abstract

A doped  $\text{Mn}_x\text{Zn}_{1-x}\text{La}_{0.1}\text{Fe}_{1.9}\text{O}_4$ ;  $0 \leq x \leq 1$  Mn–Zn ferrite was prepared by using the standard ceramic technique. The dielectric constant  $\epsilon'$ , dielectric loss factor  $\epsilon''$  and the a.c. conductivity ( $\ln \sigma$ ) were measured as a function of temperature at different frequencies. Different polarization mechanisms appeared responsible for the variation in the dielectric constant. The polarization process is favored at low frequency, whereas at high frequency alignment of dipoles is disturbed. The decrease in the internal viscosity of the system allows the dipoles to dissipate the thermal energy produced from their friction. The variation of the electrical conductivity is mainly attributed to thermally activated mobility and not to thermal creation of charge carriers. The existence of more than one straight line on the conductivity data indicates the concurrence of several conduction mechanisms. The value of the calculated activation energy indicates the semiconducting behaviour of the investigated materials. Seebeck voltage coefficients measurements indicate that electrons and holes as well as small polarons are responsible for the conduction, where in some samples the electronic conduction predominates.

© 2005 Elsevier Ltd and Techna Group S.r.l. All rights reserved.

**Keywords:** Ferrite material; Dielectric constant; Dielectric loss factor; Conductivity; Seebeck voltage coefficient

## 1. Introduction

Polycrystalline ferrites are important materials in many applications, especially in the high-frequency range due to their high dielectric constant, low losses, high resistivity and high Curie temperature [1].

Ferrites of very high dielectric constant are useful in designing microwave devices, such as isolators, circulators ..., etc. [2]. Mn–Zn ferrites are characterized by their high magnetic permeability [3].  $\text{Zn}^{2+}$  in diluted ferrites appears to change both electric and magnetic properties and promote densification and grain growth [4].

In general and according to Koops model, ferrite components are mainly formed of high-conductivity layers separated by ultra-thin insulating layer [5]. Under slightly reducing condition, the formed  $\text{Fe}^{2+}$  ions will help the conduction mechanisms where  $\text{Fe}^{2+} \leftrightarrow \text{Fe}^{3+} + \text{e}^-$ .

Rare earth ions affect drastically the physical properties of substituted Mn–Zn ferrite, because they are of larger ionic radius. When these ions enter the octahedral (B-site), they

can replace  $\text{Fe}^{3+}$  ions at low rare earth concentrations [6]. In this case, the difference in the ionic radii will lead to microstrains, which may cause domain wall motion resulting in deformed spinel structure. Ahmed et al. [7] found that the dielectric behaviour of Mn–Zn ferrite varied dramatically as a function of sintering temperature. Generally, in Mn–Zn ferrite, the Mn-cations are found on both A and B sites [8], which makes it a partially inverse spinel. The motions of cations are of great importance and affect directly the distortion of the system. In the case of La-substituted Mn–Zn ferrite, it was expected that the nonmagnetic  $\text{La}^{3+}$  ion reside at the grain boundaries, especially at relatively high concentration. So, these ions can prevent the domain wall motion, affecting both electrical and magnetic properties of the material.

## 2. Experimental techniques

The used oxides (BDH) were mixed together in stoichiometric ratios according to the formula  $\text{Mn}_x\text{Zn}_{1-x}\text{La}_{0.1}\text{Fe}_{1.9}\text{O}_4$ ;  $0 \leq x \leq 1$ . The standard ceramic technique [9] was

E-mail address: samirsolyman@hotmail.com.

used to prepare the investigated materials. Presintering was carried out at 900 °C for 30 h with heating rate of 6 °C/min using Lenton furnace 16/5 UAF (UK), then the materials were cooled to room temperature with the same rate as that of heating. The materials were grinded again and pressed to pellets and sintered at 1200 °C for 50 h with the same rate as that of presintering.

The two surfaces of each pellet were accurately polished, coated with silver paste (BDH), and checked for good conduction. The two-probe method was used for measuring the a.c. conductivity and dielectric constant using a self-calibrated Hioki LRC high tester model 3531. Seebeck voltage coefficient was measured as a function of temperature in the same range as for the electrical properties measurements. The temperature of the samples was measured using a T-type thermocouple with accuracy better than  $\pm 1$  °C.

### 3. Results and discussion

Fig. 1a–f illustrates the dependence of the dielectric constant ( $\epsilon'$ ) and the absolute temperature as a function of the applied frequency for the samples  $\text{Mn}_x\text{Zn}_{1-x}\text{La}_{0.1}\text{Fe}_{1.9}\text{O}_4$ , ( $0 \leq x \leq 1$ ). The general behaviour of the data is nearly the same with small shift in the peak position and height, depending on the frequency and Mn content. Fig. 1a indicates an increase in  $\epsilon'$  with increasing temperature giving a shoulder at about 575 K after which a spike appeared at 600 K, then decreases giving nearly stable values from 650 K and above. The difference between Fig. 1a and b in magnitude and shape of  $\epsilon'$  is mainly due to the replacement of Mn and La in the parent compound ( $\text{ZnFe}_2\text{O}_4$ ). From the figure it is clear that two humps appeared at 450 and 525 K. Minimum values of  $\epsilon'$  are obtained at about 580 K, then  $\epsilon'$

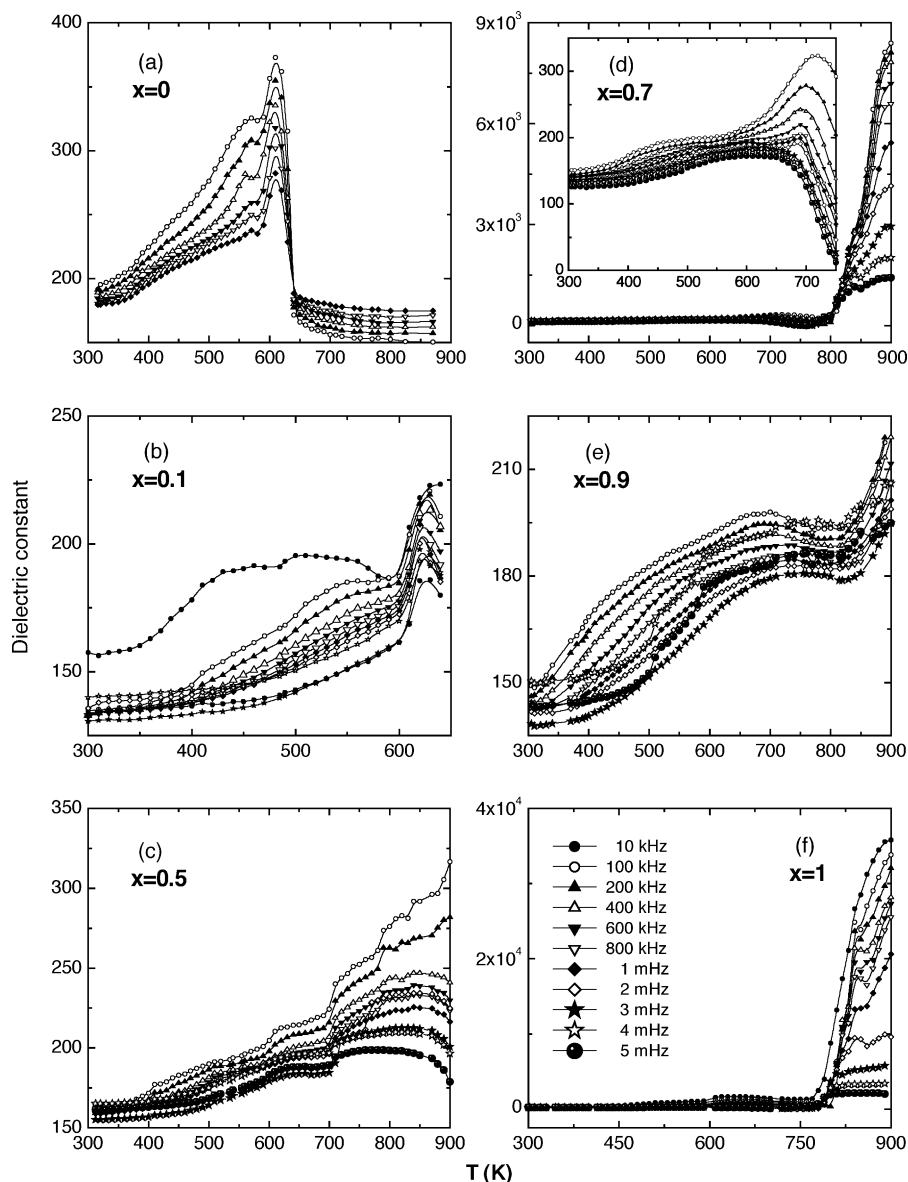


Fig. 1. (a–f) The relation between the dielectric constant  $\epsilon'$  and temperature at different frequencies for the ferrite  $\text{Mn}_x\text{Zn}_{1-x}\text{La}_{0.1}\text{Fe}_{1.9}\text{O}_4$ .

increases sharply and decreases again. This behaviour was ascribed to the presence of different types of polarization.

The electronic polarization is the most predominant one in the first temperature region. The thermal energy is too small to release the charge carriers from their localized states, giving rise to small values of  $\epsilon'$  at all Mn concentrations. The rotational, orientational and Maxwell–Wagner polarization are expected to play a role in the second temperature region (after  $\approx 420$  K). The thermal energy is quite sufficient to free more charge carriers and the field accompanied with the applied frequency orient them in its direction, though increases the polarization as well as  $\epsilon'$ . The electric dipoles cannot follow up the field variation, leading to the decrease in  $\epsilon'$  with frequency increase. Above the transition point the dielectric constant  $\epsilon'$  decreases at all frequencies. This can be attributed to the increase of lattice

vibrations, electron lattice scattering, internal friction of the dipoles and the decrease of the internal viscosity as well as the thermal energy dissipation inside the samples. Generally, the behaviour of  $\epsilon'$  can be explained on the basis of Koops theory [5] for the inhomogeneous double-layer dielectric structure [10]. The normal behaviour of a dielectric, as a function of frequencies, derives from the observation that beyond a certain high frequency of the applied a.c. electric field, the electron exchange between  $\text{Fe}^{2+}$  and  $\text{Fe}^{3+}$  ions ( $\text{Fe}^{2+} \leftrightarrow \text{Fe}^{3+} + e^-$ ) and hole transfer between  $\text{Mn}^{2+}$  and  $\text{Mn}^{3+}$  ions cannot follow up the alternating frequency of the applied field [11,12].

The variation of the dielectric loss factor  $\epsilon''$  with temperature as a function of the applied frequency is shown in Fig. 2a–f. Two distinct regions may be observed, the first one from 300 to 600 K, in which  $\epsilon''$  is frequency and

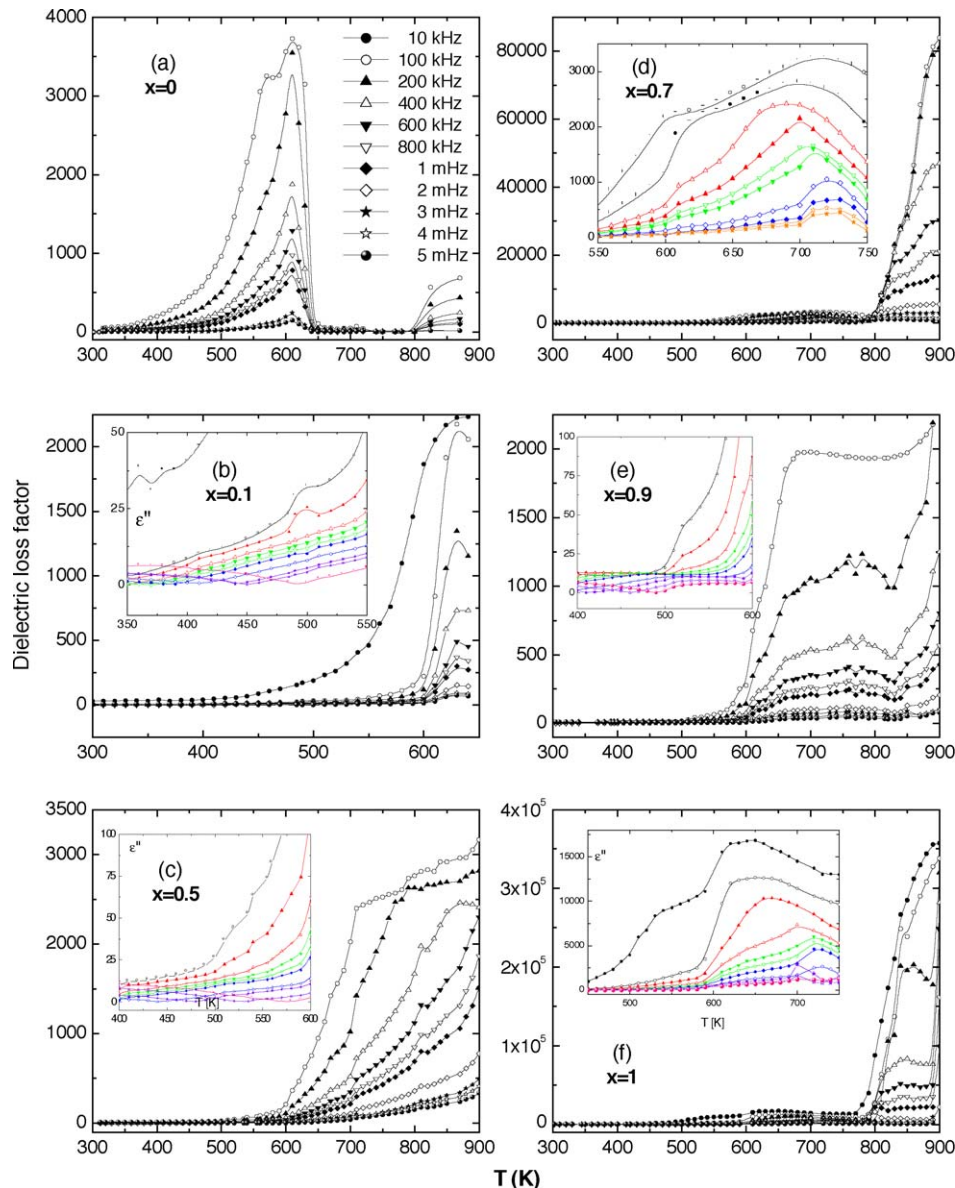


Fig. 2. (a–f) The variation of the dielectric loss factor  $\epsilon''$  as a function of temperature at different frequencies for the ferrite  $\text{Mn}_x\text{Zn}_{1-x}\text{La}_{0.1}\text{Fe}_{1.9}\text{O}_4$ .

temperature independent and a second region which is frequency and temperature dependent, in which  $\varepsilon''$  reaches a maximum value and then decreases. The dielectric loss factor  $\varepsilon''$  is decreased with increasing the applied frequency, meanwhile it increase with increasing Mn concentration, except for  $x=0.9$ . The peak was shifted towards higher temperature with increasing frequency. This means that, at low temperature, the dielectric loss factor is small, while at high temperature, the change in entropy increases with increasing temperature, i.e., the internal viscosity of the

system is decreased with heating, leading to more degrees of freedom of the dipoles. The result of this process is the increase in the friction and  $\varepsilon''$ . The increase in the entropy of the system can be attributed to the small relaxation time of  $\text{Mn}^{3+}$  ions on the octahedral site, which is based on their crystal field stabilization energy. The observed increase and decrease in  $\varepsilon''$  can be interpreted as the effect of manganese ions on the anisotropy of the material and enhancement of spin lattice relaxation rates, leading to a larger value of entropy. The decrease in  $\varepsilon''$  after the peak is attributed to the

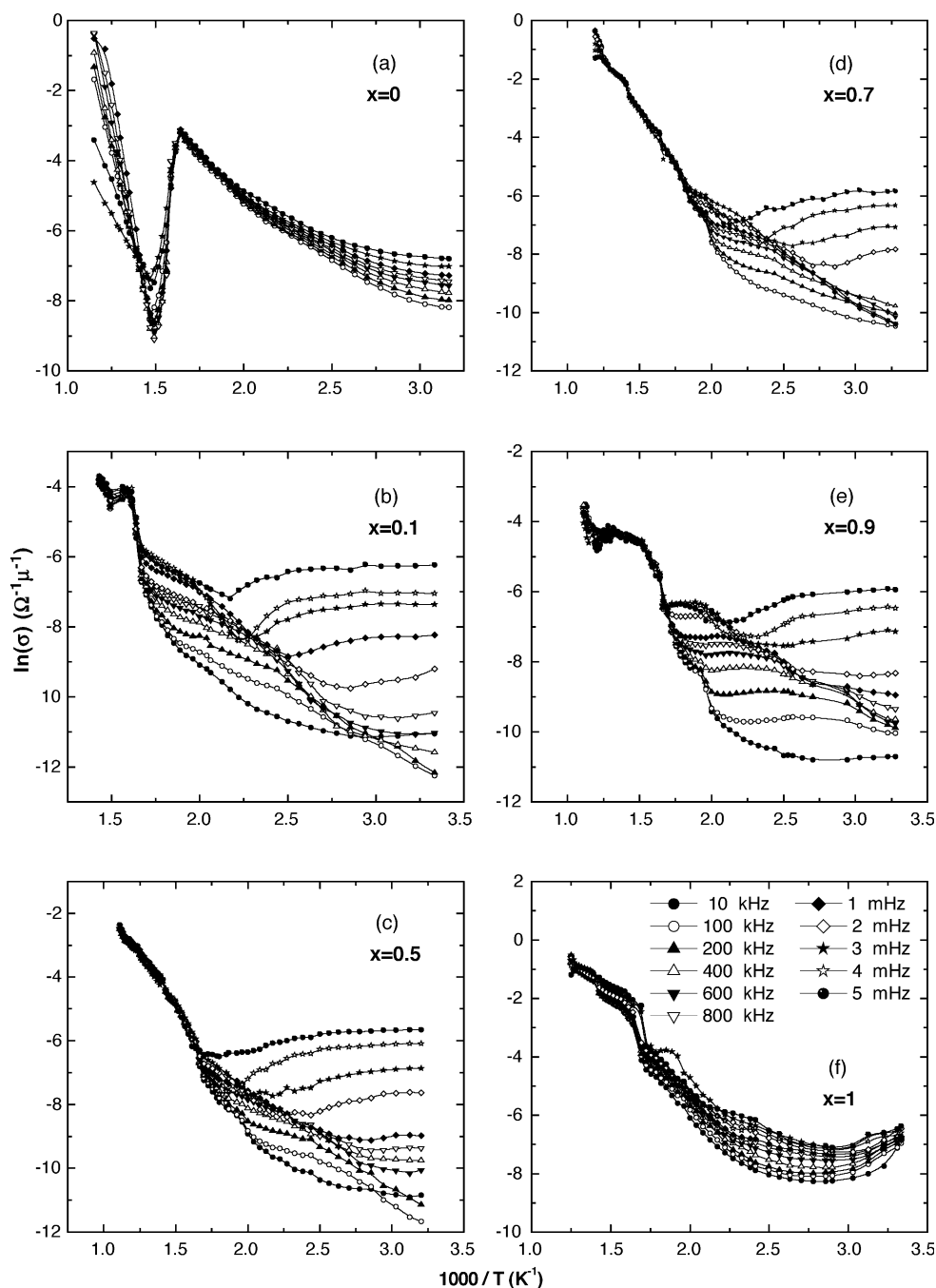


Fig. 3. (a–f) The variation of the conductivity  $\ln \sigma$  as a function of the reciprocal of absolute temperature at different frequencies for the ferrite  $\text{Mn}_x\text{Zn}_{1-x}\text{La}_{0.1}\text{Fe}_{1.9}\text{O}_4$ .

Table 1

Concentration	10 kHz	100 kHz	200 kHz	400 kHz	600 kHz	800 kHz	1000 kHz	2000 kHz	3000 kHz	4000 kHz	5000 kHz
(a) Values of the activation energy in eV at the high-temperature regions of the compound $\text{Mn}_x\text{Zn}_{1-x}\text{La}_{0.1}\text{Fe}_{1.9}\text{O}_4$											
$x = 0$	–	1.87	1.79	2.08	2.19	2.32	2.56	–	0.77	–	1.09
$x = 0.1$	0.84	0.71	0.73	0.73	0.65	0.53	0.54	0.37	0.54	0.38	0.35
$x = 0.5$	0.45	0.43	0.42	0.46	0.44	0.47	0.44	0.43	0.52	0.45	0.48
$x = 0.7$	–	0.63	0.61	0.63	0.66	0.62	0.64	0.65	0.61	0.63	0.64
$x = 0.9$	0.92	0.94	1.00	0.91	1.11	0.81	0.85	0.89	0.94	1.36	1.00
$x = 1$	0.34	0.33	0.30	0.27	0.27	0.25	0.29	0.29	0.24	0.24	0.23
(b) Values of the activation energy in eV at the low-temperature regions of the compound $\text{Mn}_x\text{Zn}_{1-x}\text{La}_{0.1}\text{Fe}_{1.9}\text{O}_4$											
$x = 0$	–	0.41	0.42	0.43	0.43	0.42	0.42	–	0.42	–	0.44
$x = 0.1$	0.31	0.21	0.18	0.17	0.17	0.17	0.23	0.25	0.25	0.26	0.19
$x = 0.5$	0.41	0.34	0.12	0.16	0.19	0.19	0.24	0.28	0.29	0.44	0.13
$x = 0.7$	–	0.31	0.19	0.17	0.14	0.15	0.15	0.24	0.25	0.33	0.38
$x = 0.9$	0.54	0.42	0.31	0.27	0.15	0.20	0.11	0.24	0.30	0.24	0.18
$x = 1$	0.25	0.29	0.25	0.25	0.16	0.14	0.14	0.19	0.17	0.21	0.14

participation of other types of polarization, such as Maxwell–Wagner polarization. Similar behaviour has been reported by other authors [13,14].

Fig. 3a–f shows the variation of a.c. conductivity ( $\ln \sigma$ ) as a function of the reciprocal of absolute temperature at different frequencies. Two distinct regions may be observed which follow the well-known Arrhenius relation  $\sigma = \sigma_0 \exp(-E_a/kT)$ , where  $\sigma_0$  is pre-exponential factor,  $E_a$  the activation energy,  $k$  the Boltzman constant and  $T$  the absolute temperature. In the first region from 300 to 500 K, no variation of  $\sigma$  with temperature was observed (metallic-like behaviour region). The second region, which extends from 500 to 600 K, is frequency and temperature dependent. The third region covers the rest of the temperature range. This region is temperature dependent and slightly frequency dependent. More than one straight line is obtained for the conductivity data, indicating the different conduction mechanisms. The hopping model is the most predominant one. The hopping process may be either electron hopping between same ions of different valencies ( $\text{Fe}^{2+} \leftrightarrow \text{Fe}^{3+} + e^-$ ) or hole hopping between Mn ions ( $\text{Mn}^{3+} \leftrightarrow \text{Mn}^{2+} + e^+$ ). The replacement of  $\text{La}^{3+}$  ions of large radius ( $R_{\text{La}^{3+}} = 1.154 \text{ \AA}$ ) than  $\text{Fe}^{3+}$  ions ( $R_{\text{Fe}^{3+}} = 0.641 \text{ \AA}$ )

on octahedral sites helps in initiating some defects that act as trapping centers for the charge carriers. So, one can expect an increase in the electrical conductivity with increasing temperature after the metallic-like behaviour region. The activation energy at low- and high-temperature regions calculated and listed in Table 1 indicates the semiconducting behaviour of the investigated samples as previously reported [15].

The variation of Seebeck voltage coefficient with the average absolute temperature for  $\text{Mn}_x\text{Zn}_{1-x}\text{La}_{0.1}\text{Fe}_{1.9}\text{O}_4$ ,  $0 \leq x \leq 1$ , materials are given in Fig. 4. The data in are classified into two groups, the first one of  $0.7 \leq x \leq 1$  while the second is for  $x < 0.7$ . The first group shows that the conduction is due to both electrons that are initiated from the valence exchange between iron ions, and the holes produced from valence exchange between Mn ions. Also in this group, it is clear that the number of charge carriers is nearly constant. This means that the variation in the conductivity is due to thermally activated mobility and not due to thermal-activated creation of charge carriers. In the second group where the Zn content is less than 0.7, the conduction is obviously due to electrons. Finally, it has to be considered that cations on A and B sites contribute to the Seebeck coefficient and so increase the conductivity of the samples.

#### 4. Conclusion

The decrease in the dielectric constant as well as the dielectric loss factor with increasing frequency is attributed to the small relaxation time of  $\text{Mn}^{3+}$  ions on the octahedral site. The effect of  $\text{Mn}^{2+}$  ions on the anisotropy of the material and the enhancement of the spin lattice relaxation rates cause an increase and decrease of  $\epsilon'$  and  $\epsilon''$  values. The hopping model is the most predominant one in the discussion of the conductivity, which is of the same origin as the dielectric properties. The replacement of  $\text{Fe}^{3+}$  ions by  $\text{La}^{3+}$  ions on octahedral site helps in initiating some defects that act as trapping centers for the charge carriers. The

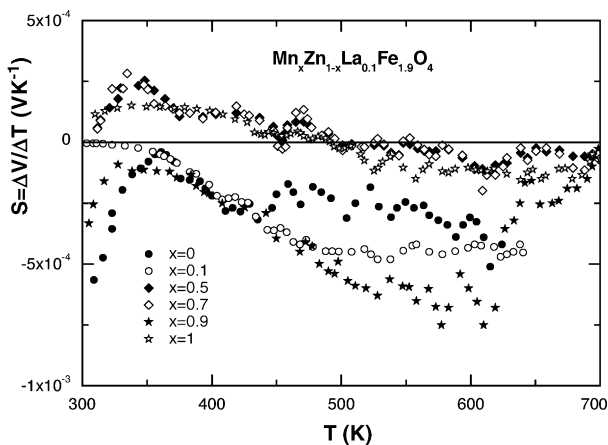


Fig. 4. Seebeck voltage coefficient as a function of the average temperature.

variation of the conductivity is due to thermally activated mobility and not to thermal-activated creation of charge carriers. The values of the activation energy indicate that the investigated samples behave like a semiconductor, though it can be called semiconducting ferrite.

## References

- [1] A.D.P. Rao, P.M.R. Rao, S.B. Raju, *Mater. Chem. Phys.* 65 (2000) 90.
- [2] D. Ravinder, A.V.R. Reddy, G.R. Mohan, *Mater. Lett.* 52 (2002) 259.
- [3] M.J. Reece, D.J. Barber, *J. Mater. Sci.* 22 (1987) 2447.
- [4] P. Kishan, D.R. Sagar, P. Swarup, *J. Less-Common Met.* 108 (1985) 345.
- [5] C.G. Koops, *Phys. Rev.* 83 (1951) 121.
- [6] E. Rezlescu, N. Rezlescu, C. Pasnicu, M.L. Craus, P.B. Popo, *Cryst. Res. Technol.* 31 (3) (1996) 343.
- [7] M.A. Ahmed, E.H. El-Khawass, F.A. Radwan, *J. Mater. Sci.* 36 (2001) 1.
- [8] G.D. Price, S.L. Price, J.K. Burdett, *Phys. Chem. Miner.* 8 (1982) 69.
- [9] M.A. Ahmed, T. Bishay Samiha, *J. Magn. Magn. Mater.* 279 (2004) 178.
- [10] J. Maxwell, *Electricity and Magnetism*, Oxford University Press, London, 1873, section 328.
- [11] V.R. Murthy, J. Sobhanaddir, *Phys. Status Solidi (a)* 36K (1976) 33.
- [12] M.A. Ahmed, S.T. Bishay, E.H.J. El-Khawass, *J. Mater. Sci. Lett.* 19 (2000) 791.
- [13] G.F. Dionne, *J. Appl. Phys.* 57 (1985) 3727.
- [14] M.A. Ahmed, M.H. Wasfy, *Indian J. Pure Appl. Phys.* 41 (2003) 731.
- [15] A.D.P. Rao, B. Ramesh, P.R.M. Rao, S.B. Raju, *Indian J. Pure Appl. Phys.* 37 (1999) 51.